

# NITRIC ACID ATTACK ON HARDENED PASTE OF GEOPOLYMERIC CEMENTS

## PART 2

ALI ALLAHVERDI, FRANTIŠEK ŠKVÁRA

*Department of Glass and Ceramics  
Institute of Chemical Technology  
Technická 5, 166 28 Prague, Czech Republic  
E-mail: Ali.Allahverdi@vscht.cz*

Submitted October 19, 2000; accepted February 1, 2001.

*Mechanism of nitric acid attack on hardened paste of geopolymeric cements, in addition to the leaching process discussed in part I [1], consists of an electrophilic attack by acid protons on polymeric Si-O-Al bonds resulting in the ejection of tetrahedral aluminium from the aluminosilicate framework. The framework vacancies are mostly re-occupied by silicon atoms resulting in the formation of an imperfect highly siliceous framework that is relatively hard but brittle. The ejected aluminium converted to octahedrally coordinated aluminium mostly accumulates in the intraframework space.*

Keywords: Geopolymeric cement, Acid attack, Fly ash, Blast furnace slag

### INTRODUCTION

Acidic corrosion of hydrated cement based materials [2, 3] has attained more importance in the recent decade due to the deteriorating effects of acidic media (e.g. acidic rains, acidic groundwaters, etc) on cement based constructions. At the same time development of geopolymeric cements (a new class of alkali-activated materials) with considerably improved properties including acid resistance necessitates more detailed investigations. Many authors [4, 5, 6] claimed that geopolymeric cements produced by activating blast furnace slag or mixtures of fly ash and blast furnace slag show an acid resistance greatly exceeding that of ordinary Portland cement. Rostami and Silverstrim [7, 8] developed an alkali-activated material called, chemically activated fly ash (CAFA), by activating Class F fly ashes. The resistance of CAFA concrete to chemical attack by acids such as sulfuric, nitric, hydrochloric, and organic acids is claimed to be far better than that of portland cement concrete [7]. According to Silverstrim *et al* [8], CAFA specimen exposed to 70% nitric acid for 3 months retained its dense microstructure.

The present work is devoted to the study of the mechanism of nitric acid attack on hardened paste of geopolymeric cements. The geopolymeric cement (for simplicity referred to as "GC") used in this work was produced according to the work of Škvára and Bohuněk [9].

### EXPERIMENTAL

The materials used for this study and the procedures for specimens preparation and test method were all discussed in part 1 [1]. The principal laboratory techniques used to study the corroded specimens include: XRD (Seifert XRD 3000P), EPMA (JEOL Superprobe 733), SEM (JEOL), MAS NMRS (BRUKER AVANCE DSX 200) and FTIRS (Nicolet 740). The results of XRD, EPMA, and SEM techniques were presented and discussed in the first part of this article [1]. The present article (part 2) is allocated to the results of MAS NMR and FTIR spectroscopy techniques.

### RESULTS AND DISCUSSION

To investigate the chemical modifications in the aluminosilicate framework during the course of corrosion process, samples of unaffected GC and its corroded layer developed after 90 days of exposure to  $pH = 1$  nitric acid were prepared and scanned by a digital solid state NMR. Solid state high resolution  $^{29}\text{Si}$  MAS NMR spectroscopy of the framework silicon atoms is a very useful tool for structural studies of aluminosilicate species (e.g. zeolites, clays, ceramics, geopolymers). In the solid insoluble aluminosilicates with tectosilicate framework the  $^{29}\text{Si}$  chemical shifts depend primarily on the degree of silicon substitution by aluminium in the lattice. Five distinct  $^{29}\text{Si}$  chemical shift ranges are thus created depending on the number of  $\text{AlO}_4$  tetrahedra connected to the  $\text{SiO}_4$  tetrahedron under consideration. Indicating in brackets the number

of aluminium tetrahedra sharing oxygen with the  $\text{SiO}_4$  tetrahedron, the five different structural units in the aluminosilicate framework include; Si(0Al), Si(1Al), Si(2Al), Si(3Al), and Si(4Al) for which characteristic  $^{29}\text{Si}$  shift ranges with about 5 ppm low-field shifts for each additional aluminium substitution [10, 11, 12]. Si(4Al) resonates at about -85 ppm and Si(0Al) at approximately -107 ppm from Tetramethylsilane (TMS) as the reference compound [13]. It should be noted that intensity distribution of the  $^{29}\text{Si}$  MAS NMR lines changes in accordance with the Si/Al ratio. In fact increasing Si/Al ratio leads to increasing intensities of  $^{29}\text{Si}$  lines corresponding to units with lower degree of substitution by aluminium [11, 12]. For Si/Al = 1 only the single Si(4Al) line is present while for Si/Al = 1.5–2 the Si(3Al) and Si(2Al) lines have the highest intensities and for Si/Al = 3–5 the Si(1Al) and Si(0Al) lines are predominant [10]. This general trend can be regarded as a further indirect proof for the assignment of the  $^{29}\text{Si}$  MAS NMR spectra of aluminosilicates.

As seen in figure 1, the unaffected sample of GC gives a  $^{29}\text{Si}$  spectrum, which is completely different than those obtained in crystalline zeolites. The spectrum consists of a broad resonance at -85 ppm along with a number of small resonances both at the lower and higher field shifts. The smaller resonances specially those at the lowest and at the highest fields, i.e. -67 and -110 ppm, are narrow which means that they relate to ordered environments different from the disordered main part of the matrix [12]. Since it is very difficult to draw reliable conclusions, the characterization of mainly amorphous GCs is quite less studied by using MAS NMR spectroscopy. The only similar spectrum is reported by Davidovits [12] for a geopolymeric binder

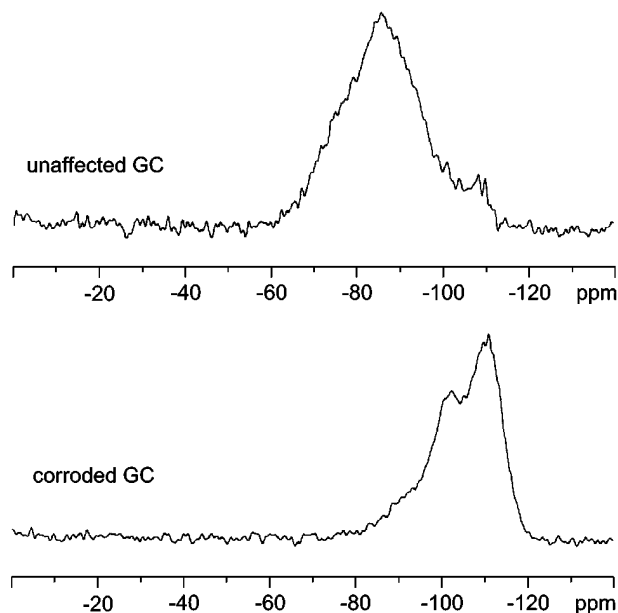


Figure 1.  $^{29}\text{Si}$  MAS NMR spectra of the geopolymeric cement and its corroded layer developed after 90 days of exposure to nitric acid at  $pH = 1$ .

called, GEOPOLYMITE. Here in spite of the lack of information in the literature and the fact that the assignment of the resonances in such a complicated spectrum is quite difficult, we try to do the task using the available information on crystalline zeolites.

A previous study [14] has shown that the chemical shift of  $^{29}\text{Si}$  in an amorphous or highly disordered environment is increased by approximately 5 ppm. The resonances found at -79, -85, -90, -95, and -101 ppm are therefore related to ordered  $^{29}\text{Si}$  chemical shifts of -84, -90, -95, -100, and -106 ppm which can be assigned to Si(4Al), Si(3Al), Si(2Al), Si(1Al), and Si(0Al) respectively. The Si/Al = 2.8 ratio therefore led to a framework consisting predominantly of Si(3Al) units. The other four structural units are also present but in smaller amounts. The resonances are markedly broadened not only due to the amorphous character of the material (broad resonances are generally found in zeolitic gels before crystallization of the zeolites [12]), but also due to the relatively low frequency of the applied magnetic field. It is well known that an increase in the frequency of the magnetic field results in considerable improvements in the quality of  $^{29}\text{Si}$  spectra of zeolites due to the removal of some field-dependent effects [11]. In addition, the effects of paramagnetic impurities, e.g.  $\text{Fe}^{3+}$ , specially in the amorphous samples on broadening the lines and producing spinning side-bands should be taken into consideration [11].

A number of small resonances specially those located at the lower and higher field shifts, e.g. at -67, -72, -75, and at -104, -108.5, -110 ppm respectively related to ordered  $^{29}\text{Si}$  chemical shifts of -72, -77, -80, and -109, -113.5, -115 ppm, can be assigned to silicates with different degree of condensation of  $\text{SiO}_4^-$  units which display a total range of chemical shifts from -60 to -120 ppm from TMS [11]. The resonances at the lower field shift can be assigned to nesosilicates ( $Q^0$ ), sorosilicates ( $Q^1$ ), inosilicates ( $Q^2$ ), and phyllosilicates ( $Q^3$ ) and those at the higher field shift can be assigned to non-equivalent Si(4Si) units in silica polymorphs ( $Q^4$ ) [15].

As seen in figure 1, the  $^{29}\text{Si}$  spectrum of the corroded sample shows a number of relatively sharp peaks at -110, -108.5, -106, and -102 ppm and a few relatively broad resonances at lower field shifts, e.g. at -100, -94.5, and -90.5 ppm. The resonances at -110, -108.5, and -106 ppm respectively related to ordered  $^{29}\text{Si}$  chemical shifts of -115, -113.5, and -111 ppm can be assigned to silica polymorphs ( $Q^4$ ) and those at -102, -94.5, -90.5 ppm respectively related to ordered  $^{29}\text{Si}$  chemical shifts of -107, -100, and -95 ppm can be attributed to Si(0Al), and residual Si(1Al) and Si(2Al) respectively. Knowing that the corroded sample contains a considerable content of quartz that was present in the unaffected GC and enriched during the process of acidic corrosion due to the leaching of the soluble contents, the resonance at about -106 ppm can also be attributed to the structural unit of quartz.

Now irrespective of the correct assignment of the resonances, a comparison of the two  $^{29}\text{Si}$  spectra of the

corroded and unaffected samples clearly shows that the process of acidic corrosion of aluminosilicate framework of GCs is an aluminium removal process in which the Si(4Al), Si(3Al), Si(2Al), and Si(1Al) structural units are dealuminated and converted to Si(0Al). The spectrum of the corroded sample clearly shows that the framework vacancies have been mostly re-occupied by silicon atoms. However a part of framework vacancies probably remained the same reflecting a range of possible environments for Si atoms including one, two or three neighboring hydroxyl groups. Knowing that in zeolites Si(3Si)(OH) groups resonate at -100 ppm and Si(2Si)(OH)<sub>2</sub> at -90.5 ppm [16], the relatively broad resonance at -100 ppm can be attributed to Si(3Si)(OH) groups and the small resonance at -90.5 ppm to Si(2Si)(OH)<sub>2</sub> coinciding with that of Si(1Al) groupings.

Compared with <sup>29</sup>Si, the MAS NMR spectrum of the other most abundant atom of the aluminosilicate frameworks, i.e. <sup>27</sup>Al, also provides useful chemical information. Müller et al [17] were the first who found that the Loewenstein rule is obeyed in aluminate and aluminosilicates anions. The Loewenstein aluminium avoidance principle states that whenever two tetrahedra are linked by one oxygen only one can be occupied by Al and there can hence be no Al-O-Al bridges [18]. The exclusion of Al-O-Al linkages limits the number of possibilities to five Q<sup>n</sup>(nSi) structural units with  $n = 0, 1, 2, 3, 4$ . However, if Si is almost all present in 4-coordination, Al can be 4- or 6-coordinated and this means that <sup>27</sup>Al MAS NMR spectra of zeolites with only two possibilities for aluminium are much simpler than their <sup>29</sup>Si MAS NMR spectra with five possible types of Si(nAl) environments for the silicon atom. In other words, <sup>27</sup>Al MAS NMR is most valuable in probing the coordination, quantity and location of Al atoms in aluminosilicates, but less useful than <sup>29</sup>Si MAS NMR for direct structural determination. Earlier investigations [11, 17] showed that in aluminosilicates, 4-coordinated aluminium resonates at about 50±20 ppm while 6-coordinated aluminium resonates at approximately 0±10 ppm from [Al(H<sub>2</sub>O)<sub>6</sub>]<sup>3+</sup>.

For a better understanding of the phenomenon, the samples of the unaffected GC and its corroded layer were also scanned for their <sup>27</sup>Al MAS NMR spectra. The resulting spectra are shown in figure 2. As seen, each of the spectra of the corroded and unaffected samples show two broad resonances, one at about 50 ppm (50.09 and 52.10 ppm respectively) and the other at approximately 0±10 ppm (12.68 and -1.73 ppm, respectively). The resonances are markedly broadened due to the relatively low frequency of the resonance. An increase in the resonance frequency however results in substantial improvements including increased intensity and symmetry as well as the reduction of the width of the peak [19]. The resonances however obviously related to both 4- and 6-coordinated aluminium show the presence of both tetrahedral and octahedral aluminium in both samples. A careful comparison of the two spectra clearly shows that the initial signal of

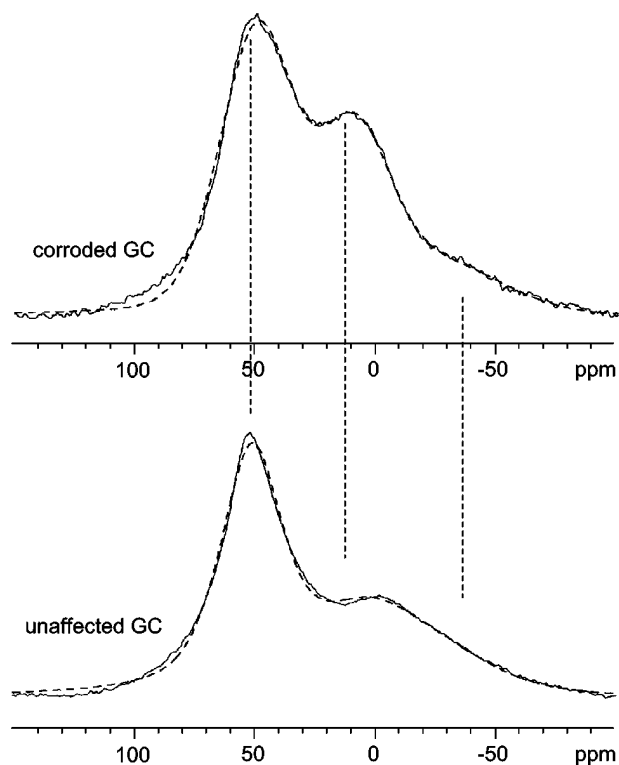


Figure 2. <sup>27</sup>Al MAS NMR spectra of the geopolymeric cement and its corroded layer developed after 90 days of exposure to nitric acid at  $pH = 1$ .

6-coordinated Al (at -1.73 ppm) in the unaffected sample has been changed to a more intensified resonance (at 12.68 ppm) in the corroded sample showing an accumulation of octahedral aluminium in the intraframework space due to ejection of tetrahedral aluminium from framework. The results of X-ray line analysis (figure 8 presented in part I) also showed that the concentration of aluminium in the corroded layer is unexpectedly high confirming that the interstitial octahedral aluminium is not removed by leaching with acid.

Since apart from MAS NMR spectroscopy, FTIR spectroscopy is also a well established technique for elucidating the structure of glassy and crystalline aluminosilicates (aluminosilicate glasses and zeolites respectively), infrared measurements were also conducted by a Nicolet 740 FTIR spectrometer. The resulting spectra of the raw materials (fly ash and blast-furnace slag) and the unaffected GC along with its corroded layers developed at  $pH = 1$  and 2 of nitric acid solutions are presented respectively in figures 3 and 4. As can be seen, the spectra of the corroded layers are very similar to the spectrum of the original unaffected GC. A comparison of these spectra to those presented in the literature for amorphous aluminosilicate glasses [20, 21] and relatively highly crystalline zeolites [22, 23, 24] reveals that they are more similar to those of amorphous aluminosilicate glasses than those of

relatively well crystalline zeolites. In fact in the case of solids with a glassy structure usually the infrared absorption peaks are not well defined and sharp as in the case of solids with an ordered structure.

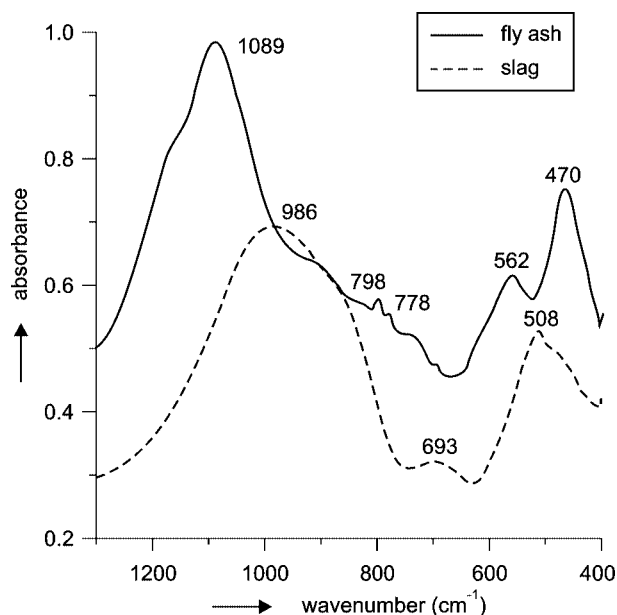


Figure 3. FTIR spectra of fly ash and blast-furnace slag.

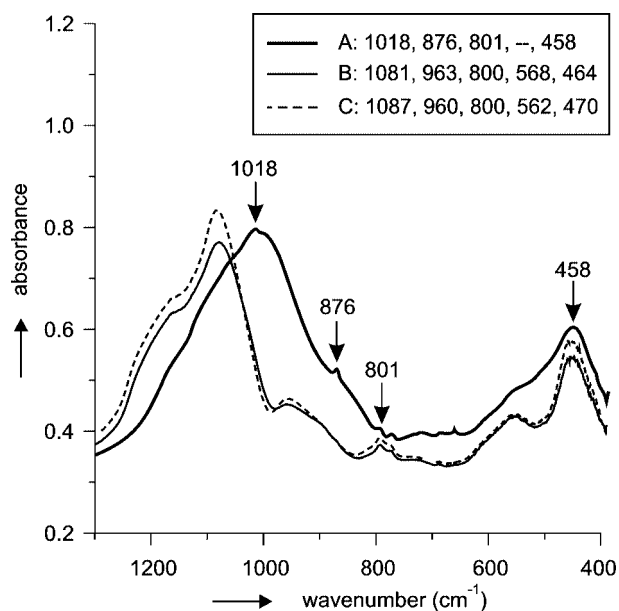


Figure 4. FTIR spectra.

A - Geopolymeric cement (alkali-activated ash/slag mixture after 24 hrs in mould at 95% relative humidity at 20 °C, followed by a hydrothermal curing and 27 days of dry cure), B - Corroded layer of the geopolymeric cement developed after 90 days of exposure to nitric acid at  $pH = 2$ , C - Corroded layer of the geopolymeric cement developed after 90 days of exposure to nitric acid at  $pH = 1$ .

As seen in figure 4, in each of the spectra of the unaffected GC and both of the corroded layers, there is a main broad and strong absorption peak appearing at 1018, 1081, and 1087  $cm^{-1}$ , a fairly broad and relatively strong peak at 458, 464, and 470  $cm^{-1}$ , a weak peak at 801, 800, and 800  $cm^{-1}$ , and a relatively weak peak at 876, 963, and 960  $cm^{-1}$  respectively. In addition to all the above peaks, the spectrum of the unaffected GC shows a shoulder at 560  $cm^{-1}$  and the spectra of the corroded layers each shows a shoulder at approximately 1170  $cm^{-1}$  and one more peak at about 560  $cm^{-1}$ .

Assignment of vibrational frequencies in aluminosilicate structures is not an easy matter and it has been a subject of controversy for many years. Many authors have reported infrared spectra of zeolites [22 - 24] and aluminosilicate glasses [25 - 28] and tried to interpret the observed bands in relation to the corresponding structure. The general agreement is that all the aluminosilicate glasses generally exhibit at least three absorption peaks including a main broad and strong absorption peak at about 1080  $cm^{-1}$ , a fairly broad and relatively strong peak at about 460  $cm^{-1}$  and a relatively weak and variable (depending on the composition) peak at about 800  $cm^{-1}$ . The first of these bands which is the most intensive is usually a superposition of some bands situated close to each other. In some cases another weak band appears at about 850 to 950  $cm^{-1}$ . The same features can be seen in the present study.

In the interpretation of infrared spectra of silicate and aluminosilicate glasses different models have been used. In the model of Bell and Dean [29] for silica polymorphs, the bent "molecule" Si-O-Si is used as a monomeric unit instead of  $[SiO_4]$  tetrahedron. This triatomic bent  $Si_2O$  units with partial substitution of Si by Al was successfully used by Handke *et al* [30] and Stoch *et al* [21] for studying vibrational spectroscopy of different silicate and aluminosilicate glasses. They assigned the general bands of all glass spectra (at about 1080, 800, 460  $cm^{-1}$ ) to stretching, bending, and rocking vibrations of the bridging oxygen atom respectively. Another model which has been extensively used for both zeolites and glasses is the tetrahedron  $SiO_4$  model in which it is assumed that one silicon atom is at the center and four oxygen atoms are at the corners of a tetrahedron and the structure represent a three dimensionally polymerized network formed by covalent Si-O-Si bands. Based on this model many authors [20, 25 - 28] assigned the strong band at about 1080  $cm^{-1}$  in silica polymorphs, alkali and lead silicates, and alkali-aluminosilicates to the Si-O bond stretching motion in  $SiO_4$  tetrahedron. It is also repeatedly reported that as the aluminium is introduced in place of silica, the peak at 1080  $cm^{-1}$  gradually shifts to a lower frequency [20, 21, 25 - 28]. The authors emphasized that the gradual shifting characteristic of this band with gradual increase in aluminium concentration confirms that this band is due to a predominant character of Si-O stretching vibrations with aluminium playing the role of perturbation. Bimalendu [20] studying infrared spectro-

scopy of aluminosilicate glasses reported that at 90 mol.% SiO<sub>2</sub> the band frequency increases to about 1100 cm<sup>-1</sup>, a value very close to the Si-O vibration frequency in glassy SiO<sub>2</sub> suggesting that probably there are very few or no coupled (Si,Al)-O vibration. This is another reason for assigning the 1080 cm<sup>-1</sup> band to the Si-O stretching motion modified by the aluminium as a cation coordinating the oxygen.

Many authors [20, 31, 32] assigned the band at about 800 cm<sup>-1</sup> to distinct stretching vibrations of the Al-O bonds in the AlO<sub>4</sub> tetrahedron which are formed in the silicon sites by ordering of aluminium. Bimalendu [20] reported that as the aluminium concentration increases, the 800 cm<sup>-1</sup> band continues to grow stronger implying that this band is dependent on the amount of substituted aluminium. The 460 cm<sup>-1</sup> band in all the glasses which is identical to that found in the spectra of silica polymorphs in this region has been assigned to the oxygen linkage to either SiO<sub>4</sub> or AlO<sub>4</sub> tetrahedra [20, 25 - 28]. Several researchers [33, 34] reported that silicates with closed rings of SiO<sub>4</sub> tetrahedra exhibit intense infrared bands in the region 800 to 950 cm<sup>-1</sup>. Such bands also appear due to non-bridging oxygens [20].

In the case of zeolites also much effort have been devoted for characterizing their structures. According to Flanigen *et al* [22], in addition to a typical infrared pattern for each zeolite species, there are often general similarities among the spectra of zeolites. The infrared spectra of zeolites in the 1300 - 200 cm<sup>-1</sup> region appears to consists of 2 classes of vibrations: those caused by internal vibrations of the framework TO<sub>4</sub> tetrahedron, the primary building unit in all zeolite framework which tend to be insensitive to variations in framework structure, and vibrations related to external linkages which are sensitive to topology (arrangement of TO<sub>4</sub>) and to the type of building unit present. In contrary to authors assigning distinct Al-O vibrations, no vibrations specific to AlO<sub>4</sub> tetrahedra or Al-O bonds are assigned but rather vibrations of TO<sub>4</sub> groups and T-O bonds where the vibrational frequencies represent the average Si,Al composition and bond characteristics of the central T cation. Flanigen *et al* [22] mentioned that the relative concentration of Si and Al in site T affects the frequency of the band and not the number of bands. This is analogous to the crystallographic equivalency of Si and Al in the T site encountered in X-ray diffraction analysis where the T-O bond distances reflect the average Si,Al composition.

#### Internal Tetrahedra;

Asymmetric stretch	1250 - 950 cm <sup>-1</sup>
Symmetric stretch	720 - 650 cm <sup>-1</sup>
T-O bend	500 - 420 cm <sup>-1</sup>

#### External Linkages;

Double ring	650 - 500 cm <sup>-1</sup>
Pore opening	420 - 300 cm <sup>-1</sup>
Symmetric stretch	820 - 750 cm <sup>-1</sup>
Asymmetric stretch	1150-1050 cm <sup>-1</sup>

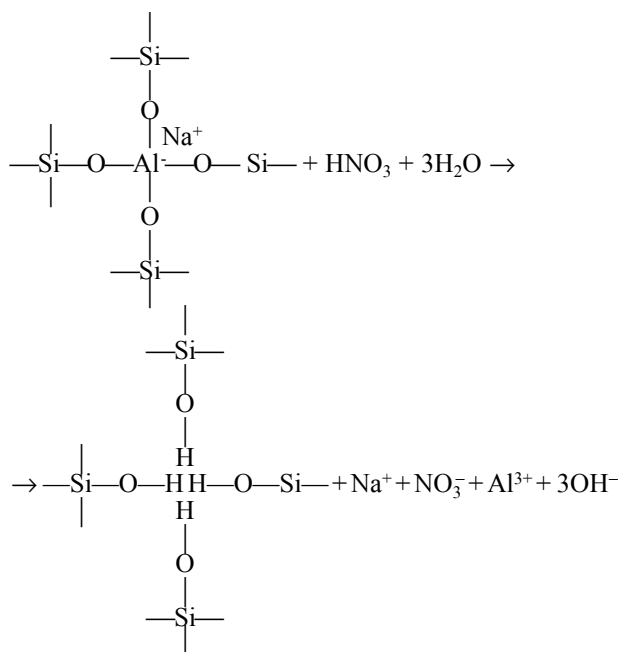
Flanigen *et al* [22] based on the comprehensive work of Lippincott *et al* [35] on the infrared spectra of the polymorphs of silica assigned the strongest vibration in the 950 - 1250 cm<sup>-1</sup> region to a T-O asymmetric stretch (motion primarily associated with oxygen atoms) and the next strongest band in the region 420 - 500 cm<sup>-1</sup> to a T-O bending mode. The symmetric stretch modes are classified into an internal tetrahedron stretch in the lower spectral region of 650 - 720 cm<sup>-1</sup> and an external linkage symmetric stretch reflecting structure sensitive external linkage in the higher region of 750 - 820 cm<sup>-1</sup>. All the stretching modes are sensitive to framework Si/Al composition and shift to a lower frequency with increasing Al content. The external linkage frequencies which are sensitive to topology and building units in the zeolite frameworks occurring in the two regions of 650-500 cm<sup>-1</sup> and 420-300 cm<sup>-1</sup> are assigned to the presence of a double ring polyhedra and a breathing motion of the isolated rings forming the pore opening in zeolites respectively. The infrared band appearing as a shoulder at about 1050 - 1150 cm<sup>-1</sup> in the asymmetric stretch region on the high frequency side of the principal T-O stretch band and showing characteristics related to framework topology assigned to external linkage asymmetric stretch. The variations in the features of this shoulder including intensity, shape and multiplicity appear to be related to framework structure characteristics.

Now irrespective of the precise assignment of the bands which requires the study of a large number of samples, the following conclusions can be drawn up confidently;

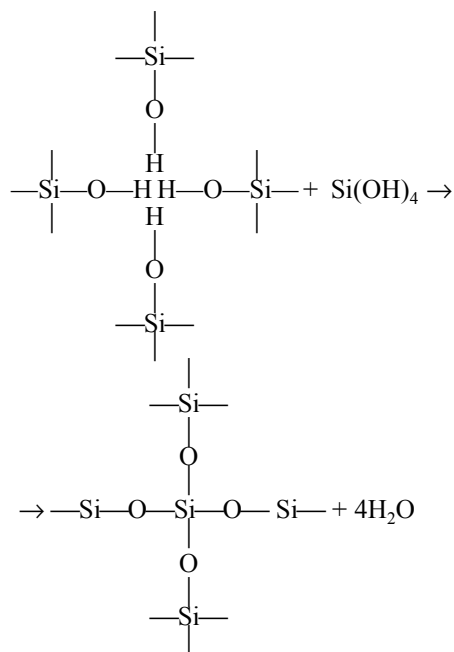
- All the absorption peaks usually observed in the spectra of aluminosilicate glasses and most of those present in the spectra of zeolites can be seen in the spectra of GC and its corroded layers (figure 4) implying the similarity between these materials.
- All the bands are quite broad implying that the structures of GC and its corroded layers are not ordered and contain varying degree of disorder of aluminium and silicon. The structures of GC and its corroded layers therefore are more similar to aluminosilicate glasses than crystalline zeolites.
- The presence of infrared bands assigned to both internal and external linkages of the TO<sub>4</sub> tetrahedra in the spectra of the corroded layers implies that a 90-days period of severe acid attack does not result in complete destruction of the framework. The ejection of tetrahedral aluminium from the aluminosilicate framework in the process of acidic corrosion and due to an electrophilic attack by acid protons on polymeric Si-O-Al bonds shifts the position of stretching modes to a higher frequency.

Now based on the information obtained from XRD, EPMA (presented in part I [1]) and in particular spectroscopy techniques of MAS NMR and FTIR, the total corrosion reaction can be postulated to occur via the following steps;

1. The first step starts by a leaching process in which sodium and calcium (charge compensating cations in the aluminosilicate framework) are exchanged by  $H^+$  or  $H_3O^+$  ions from solution along with an electrophilic attack by acid protons on polymeric Si-O-Al bonds resulting in the ejection of tetrahedral aluminum from the aluminosilicate framework;



2. In the second step the framework vacancies are mostly re-occupied by silicon atoms resulting in the formation of an imperfect highly siliceous framework. The ejected aluminium converted to octahedrally coordinated aluminium mostly accumulates in the intraframework space.



The above chemical conversions are similar to those proposed for the process of dealumination of zeolites. In crystalline zeolites the presence of channels provides the possibility for removing octahedrally coordinated interstitial aluminium by washing with acid. Zeolites can be dealuminated by prolonged acid leaching, hydrothermal treatment, and other chemical means. During dealumination, thermal stability of zeolites is considerably increased while the product retains the topology and crystallinity of the parent structure. The process is also known as ultra-stabilization since the product retains its crystallinity at temperatures in excess of  $1000^\circ\text{C}$  while the decomposition of the sodium from the zeolite takes place at about  $800^\circ\text{C}$ .

It should be considered that in spite of much effort has been devoted to the study of the dealumination process, but still a number of questions remained unanswered. The most important question is for the origin of required Si in step 2.

## CONCLUSION

The mechanism of nitric acid attack on hardened paste of geopolymeric cements, in addition to the leaching process in which sodium and calcium ions are depleted and exchanged by  $H^+$  or  $H_3O^+$  ions from the acid solution (discussed in part 1 [1]), consists of an electrophilic attack by acid protons on polymeric Si-O-Al bonds resulting in the ejection of tetrahedral aluminium from the aluminosilicate framework. The framework vacancies are mostly re-occupied by silicon atoms resulting in the formation of an imperfect highly siliceous framework. The ejected aluminium converted to octahedrally coordinated aluminium mostly accumulates in the intra-framework space.

## Acknowledgement

*This study was part of the research project CEZ: MSM 223100002 Chemistry and technology of materials for technical applications, health and environment protection.*

## References

1. Allahverdi A., Škvára F.: *Ceramics-Silikáty* 45, 81 (2001).
2. Allahverdi A., Škvára F.: *Ceramics-Silikáty* 44, 114 (2000).
3. Allahverdi A., Škvára F.: *Ceramics-Silikáty* 44, 152 (2000).
4. Changgao L., Ruihua L.: *Proc. 10<sup>th</sup> Int. Cong. Chem. Cement, Vol.4, 4iv028, Gothenburg, Sweden 1997.*
5. Blaakmeer J.: *Adv. Cem. Based Mater. 1*, 275 (1994).
6. Xincheng P., Changhui Y., Fan L.: *Proc. 2<sup>nd</sup> Int. Conf., p.717, Kyiev, Ukraine 1999.*
7. Rostami H., and Silverstrim T.: *Proc. Annual. 13<sup>th</sup> Int. Pittsburgh Coal Conf., Vol. 2, p.1074-1079, Pittsburgh 1996.*
8. Silverstrim T., Rostami H., Clark B., Martin J.: *Proc. 19<sup>th</sup> Int. Conf. Cem. Microsc., p.355, Int.Cement Microscopy Assoc. 1997.*

9. Škvára F., Bohuněk J.: *Ceramics-Silikáty* 43, 111 (1999).
10. Lippmaa E., Mägi M., Samoson A., Tarmak M., Engelhardt G.: *J. Am. Chem. Soc.* 103, 4992 (1981).
11. Klinowski J. in: *Progress in NMR Spectroscopy*, Vol. 16, p. 237-309, 1984.
12. Davidovits J.: *J. Materials Education* 16, 91 (1994).
13. Lippmaa E., Mägi M., Samoson A., Tarmak M., Engelhardt G., Grimmer A. R.: *J. Am. Chem. Soc.* 102, 4889, (1980).
14. Loewenstein W.: *Am. Mineral.* 39, 92 (1954).
15. Mägi M., Lippmaa E., Samoson A., Engelhardt G., Grimmer A. R.: *J. Phys. Chem.* 88, 1518 (1984).
16. Engelhardt G., Lohse U., Samoson A., Mägi M., Tarmak M., Lippmaa E.: *Zeolites* 2, 59 (1982).
17. Müller D., Gressner W., Behrens H. J., Scheler G.: *Chem. Phys. Lett.* 79, 59 (1981).
18. Loewenstein W.: *Am. Mineral.* 39, 92 (1954).
19. Fyfe C. A., Gobbi G. C., Hartman J. S., Klinowski J., Thomas J. M.: *Phys. Chem.* 86, 1274 (1982).
20. Bimalendu N.R.: *J. Am. Ceram. Soc.* 73, 846 (1990).
21. Stoch L., Sorda M.: *J. Mol. Struct.* 511-512, 77 (1999).
22. Flanigen E.M., Khatami H., Szymanski H.A. in: *Molecular Sieve Zeolites-I*, p.201-228, The American Chemical Society, Washington DC 1971.
23. Pichat P., Beaumont R., Barthomeuf D.: *J. Chem. Soc., Far. Trans. I.* 70, 1402 (1974).
24. Barthomeuf D.: *Zeolite Microporous Solids: Synthesis, Structure, and Reactivity*, p.193-223, Kluwer Academic Publishers, Netherlands 1992.
25. Šimon I., and McMahon H.O.: *J. Am. Ceram. Soc.* 36, 160 (1953).
26. Koloseva V.A.: *Opt.Spectrosc.* 10, 209 (1961) (Engl. Transl.).
27. Murthy M.K., Kirby E.M.: *J. Am. Ceram. Soc.* 45, 324 (1962).
28. Hanna R., Su G.J.: *J. Am. Ceram. Soc.* 47, 597 (1964).
29. Bell R.J., Dean P.: *Disc. Faraday Soc.* 50, 55 (1970).
30. Handke M., Mozgawa W.: *Vibrational Spectrosc.* 5, 75 (1993).
31. Koloseva V.A.: *Izv. Akad. Nauk. SSSR, Neorg. Mater.* 1, 442 (1965) (Engl. Trans.),
32. Day D.E., Rindone G.E.: *J. Am. Ceram. Soc.* 45, 489 (1962).
33. Saksena B.D., Agarwal K.C., Jauhri G.S.: *Trans. Faraday Soc.* 59, 276 (1963).
34. White W.B.: *Structural Interpretation of Lunar and Terrestrial Minerals by Raman Spectroscopy*, Ed. Clarence Karr Jr., Academic Press, New York 1975.
35. Lippincott E. R., Van Valkenberg A., Weir C.E., Bunting E.N.: *J. Res. Natl. Bur. Std.* A61, 61, 1958.

---

KOROZE ZATVRDLÝCH KAŠÍ GEOPOLYMERNÍCH  
CEMENTŮ ROZTOKY HNO<sub>3</sub>,  
ČÁST 2

ALI ALLAHVERDI, FRANTIŠEK ŠKVÁRA

*Vysoká škola chemicko-technologická  
Ústav skla a keramiky  
Technická 5, 166 28 Praha*

Mechanismus koroze zatvrdlé kaše geopolymerních cementů kyselinou dusičnou spočívá mimo procesu vyluhování zmíněného v části 1 [1] rovněž v elektrofilním působení kyselinových protonů na polymerní vazby Si-O-Al, způsobujícím vypuzování tetraedrového hliníku z aluminosilikátové struktury. Uvolněná místa ve struktuře jsou většinou znovu obsazena křemíkovými atomy, čímž vzniká nedokonalá vysoce křemičitá struktura, která je relativně tvrdá, avšak křehká. Vypuzený hliník, přeměněný na oktaedrově koordinovanou formu, se většinou hromadí ve vnitřních dutinách struktury.